



Tuning metal–carboxylate coordination in crystalline metal–organic frameworks through surfactant media



Junkuo Gao^{a,1}, Kaiqi Ye^{a,b,1}, Mi He^c, Wei-Wei Xiong^a, Wenfang Cao^a, Zhi Yi Lee^a, Yue Wang^b, Tom Wu^c, Fengwei Huo^a, Xiaogang Liu^{d,e}, Qichun Zhang^{a,*}

^a School of Materials Science and Engineering, Nanyang Technological University, Singapore 639798, Singapore

^b State Key Laboratory of Supramolecular Structure and Materials, Jilin University, Changchun 130012, China

^c Division of Physics and Applied Physics, School of Physical and Mathematical Sciences, Nanyang Technological University, Singapore 637371, Singapore

^d Department of Chemistry, National University of Singapore, Singapore 117543, Singapore

^e Institute of Materials Research Engineering, Agency for Science, Technology and Research, Singapore 117602, Singapore

ARTICLE INFO

Article history:

Received 23 May 2013

Received in revised form

18 July 2013

Accepted 28 July 2013

Available online 2 August 2013

Keywords:

Metal–organic frameworks

Surfactant–thermal condition

Crystalline

Structure

Magnetic property

Coordination

ABSTRACT

Although it has been widely demonstrated that surfactants can efficiently control the size, shape and surface properties of micro/nanocrystals of metal–organic frameworks (MOFs) due to the strong interactions between surfactants and crystal facets of MOFs, the use of surfactants as reaction media to grow MOF single crystals is unprecedented. In addition, compared with ionic liquids, surfactants are much cheaper and can have multifunctional properties such as acidic, basic, neutral, cationic, anionic, or even block. These factors strongly motivate us to develop a new synthetic strategy: growing crystalline MOFs in surfactants. In this report, eight new two-dimensional (2D) or three-dimensional (3D) MOFs have been successfully synthesized in an industrially-abundant and environmentally-friendly surfactant: polyethylene glycol-200 (PEG-200). Eight different coordination modes of carboxylates, ranging from monodentate η^1 mode to tetra-donor coordination $\mu_3\text{-}\eta^1:\eta^2:\eta^1$ mode, have been founded in our research. The magnetic properties of Co-based MOFs were investigated and MOF NTU-Z6b showed a phase transition with a Curie temperature (T_c) at 5 K. Our strategy of growing crystalline MOFs in surfactant could offer exciting opportunities for preparing novel MOFs with diverse structures and interesting properties.

© 2013 Elsevier Inc. All rights reserved.

1. Introduction

Metal–organic frameworks (MOFs) have attracted huge attentions due to their promising applications in gas storage [1–4], separation [5–8], catalysis [9–11], sensors [12–17] and biology [18–20]. Various synthetic methods such as hydrothermal, solvothermal, ionothermal, and urea-thermal methods have been explored to synthesize MOFs with complex structures and fascinating properties [21–24]. However, previous methods have significant limitations associated with the use of solvents. The reaction temperature has to be kept low as most of solution processes (e.g. hydrothermal, solvothermal, and urea-thermal methods) involve the use of low-boiling-point solvents. Additionally, organic solvents are a health and environmental concern. Although green solvents such as ionic liquids have been used in the synthesis of

MOFs [25–30], they have had limited scope for large-scale fabrication because of their high cost.

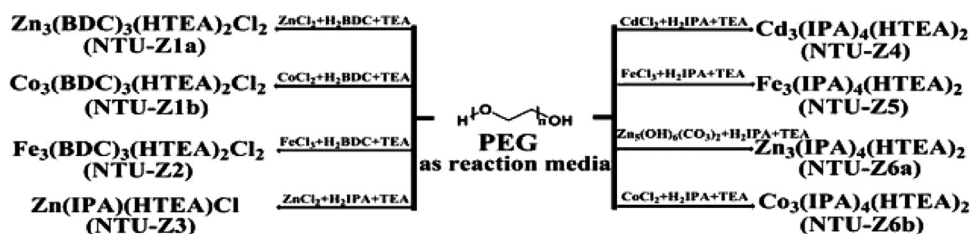
As surfactants have been widely demonstrated to efficiently control the sizes, shapes, and surface properties of nanocrystals, and the pore sizes and phases of porous frameworks [31–37], we reason that the surfactants can be used to control the growth of crystalline materials. Notably, compared with ionic liquids, the surfactants not only have high chemical and thermal stability and low vapor pressure, but also display multifunctional properties such as acidic, basic, neutral, anionic, cationic, etc. Furthermore, a large collection of surfactants are generally low cost and readily accessible. Although our group recently reported that crystalline chalcogenides can be grown under surfactant-thermal condition [38,39], the use of surfactants as reaction media to control the growth of MOF crystals is still rare [40]. Here we report a general method for controlling the growth of crystalline MOFs in surfactant media. We discover that the surfactant enables tuning of metal–carboxylate coordination, resulting in the formation of a wide range of previously inaccessible MOFs.

The selection of surfactants in this research is based on their melting point, charge, and ability to coordinate with metals. As a

* Corresponding author. Fax: +65 67909081.

E-mail address: qc Zhang@ntu.edu.sg (Q. Zhang).

¹ Both authors have equal contribution to this paper.



Scheme 1. Synthesis of eight new crystalline MOFs in surfactant PEG-200.

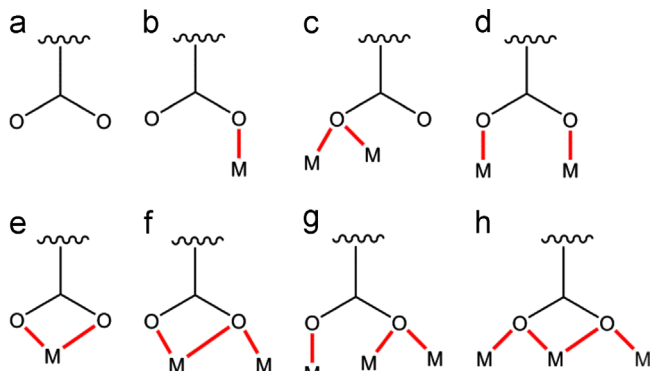


Fig. 1. Eight different coordination modes of carboxylate groups found in MOFs NTU-Z1-Z6: (a) η^0 , (b) η^1 mode, (c) μ_2 - η^2 mode, (d) μ_2 - η^1 : η^1 mode, (e) chelating η^2 mode, (f) μ_2 - η^2 : η^1 mode, (g) μ_3 - η^1 : η^2 mode, and (h) μ_3 - η^1 : η^2 : η^1 mode.

proof-of-concept experiment, polyethylene glycol (PEG) was chosen as the reaction medium because (i) PEG has been widely used in materials science for shape-controlled growth of nanoparticles and in medicinal chemistry; (ii) PEG is a biodegradable polymer with low toxicity; (iii) PEG has various melting points with the change of the weight; and (iv) PEG has many oxygen atoms suitable for bonding with metal atoms [20,41–46].

In a typical experiment, we examined surfactant (PEG-200) as the solvent and 1,4-benzenedicarboxylate acid (H_2BDC) or isophthalic acid (H_2IPA) as the ligand to construct MOFs. Eight new 2D or 3D crystal structures were prepared under similar reaction conditions (Scheme 1). Interestingly, eight different coordination modes of carboxylate groups, ranging from no binding with metal, to monodentate η^1 mode, and to tetra-donor coordination μ_3 - η^1 : η^2 : η^1 mode, have been found in our studies (Fig. 1). It is noteworthy that no crystals were obtained for all the reaction systems when PEG-200 was removed or replaced by an organic solvent such as ethylene glycol, methanol and *N,N*-dimethylformamide.

2. Experimental section

2.1. Materials and general methods

All chemicals were purchased from Alfa Aesar, TCI chemical and Aldrich and used without further purification. Polyethylene glycol 200 (PEG 200) were purchased from Alfa Aesar. Powder X-ray diffraction data were recorded on a Bruker D8 Advance diffractometer with a graphite-monochromatized $CuK\alpha$ radiation. FTIR spectra were recorded from KBr pellets by using a Perkin Elmer FTIR SpectrumGX spectrometer. Thermogravimetric analysis (TGA) was carried out on a TA Instrument Q500 Thermogravimetric Analyzer at a heating rate of 10 °C/min up to 800 °C under N_2 atmosphere. The DC magnetic susceptibility measurements were made on an MPMS magnetometer at temperatures between 2.0 and 300 K.

2.2. Synthesis

2.2.1. Synthesis of $(HTEA)_2[Zn_3(BDC)_3Cl_2]$ (NTU-Z1a)

A mixture of $ZnCl_2$ (3 mmol, 0.41 g), H_2BDC (3 mmol, 0.35 g), triethylamine (TEA) (1 mL), and 4 mL PEG-200 was put into a 30 mL Teflon-lined stainless-steel autoclave and heated at 160 °C for 6 days. Then, the mixture was naturally cooled to room temperature and washed with methanol to give colorless crystals of NTU-Z1a. Yield: 52% (based on H_2BDC). CCDC number: 921229.

2.2.2. Synthesis of $(HTEA)_2[Co_3(BDC)_3Cl_2]$ (NTU-Z1b)

A mixture of $CoCl_2 \cdot 6H_2O$ (1 mmol, 0.24 g), H_2BDC (3 mmol, 0.35 g), TEA (1 mL), and 4 mL PEG-200 was put into a 30 mL Teflon-lined stainless-steel autoclave and heated at 160 °C for 6 days. Then, the mixture was naturally cooled to room temperature and washed with methanol to give purple crystals of NTU-Z1b. Yield: 46% (based on $CoCl_2 \cdot 6H_2O$). CCDC number: 921230.

2.2.3. Synthesis of $(HTEA)_2[Fe_3(BDC)_3Cl_2]$ (NTU-Z2)

A mixture of $FeCl_3 \cdot 6H_2O$ (2 mmol, 0.54 g), H_2BDC (4 mmol, 0.46 g), TEA (1 mL), and 4 mL PEG-200 was put into a 30 mL Teflon-lined stainless-steel autoclave and heated at 160 °C for 6 days. Then, the mixture was naturally cooled to room temperature and washed with methanol to give yellow crystals of NTU-Z2. Yield: 31% (based on $FeCl_3$). CCDC number: 921231.

2.2.4. Synthesis of $(HTEA)[Zn(IPA)Cl]$ (NTU-Z3)

A mixture of $ZnCl_2$ (4 mmol, 0.54 g), H_2IPA (4 mmol, 0.46 g), TEA (1 mL), and 4 mL PEG-200 was put into a 30 mL Teflon-lined stainless-steel autoclave and heated at 160 °C for 6 days. Then, the mixture was naturally cooled to room temperature and washed with methanol to give colorless crystals of NTU-Z3. Yield: 61%. CCDC number: 921232.

2.2.5. Synthesis of $(HTEA)_2[Cd_3(IPA)_4]$ (NTU-Z4)

A mixture of $CdCl_2$ (3 mmol, 0.55 g), H_2IPA (5 mmol, 0.58 g), TEA (2 mL), and 5 mL PEG-200 was put into a 30 mL Teflon-lined stainless-steel autoclave and heated at 160 °C for 6 days. Then, the mixture was naturally cooled to room temperature and washed with methanol to give colorless crystals of NTU-Z4. Yield: 55% (based on $CdCl_2$). CCDC number: 921233.

2.2.6. Synthesis of $(HTEA)_2[Fe_3(IPA)_4]$ (NTU-Z5)

A mixture of $FeCl_3 \cdot 6H_2O$ (2 mmol, 0.54 g), H_2IPA (4 mmol, 0.46 g), TEA (1 mL), and 4 mL PEG-200 was put into a 30 mL Teflon-lined stainless-steel autoclave and heated at 160 °C for 6 days. Then, the mixture was naturally cooled to room temperature and washed with methanol to give orange crystals of NTU-Z5. Yield: 34% (based on $FeCl_3 \cdot 6H_2O$). CCDC number: 921234.

2.2.7. Synthesis of $(HTEA)_2[Zn_3(IPA)_4]$ (NTU-Z6a)

A mixture of $Zn_5(OH)_6(CO_3)_2$ (1 mmol, 0.55 g), H_2IPA (4 mmol, 0.46 g), TEA (1 mL), and 4 mL PEG-200 was put into a 30 mL Teflon-lined stainless-steel autoclave and heated at 160 °C for

6 days. Then, the mixture was naturally cooled to room temperature and washed with methanol to give colorless crystals of **NTU-Z6a**. Yield: 58% (based on H₂IPA). CCDC number: 921235.

2.2.8. Synthesis of (HTEA)₂[CO₃(IPA)₄] (**NTU-Z6b**)

A mixture of CoCl₂·6H₂O (1 mmol, 0.24 g), H₂IPA (2 mmol, 0.23 g), TEA (1 mL), and 4 mL PEG-200 was put into a 30 mL Teflon-lined stainless-steel autoclave and heated at 160 °C for 6 days. Then, the mixture was naturally cooled to room temperature and washed with methanol to give purple crystals of **NTU-Z6b**. Yield: 46% (based on CoCl₂·6H₂O). CCDC number: 921236.

2.3. Single-crystal structure determination

Data collection of crystals was carried out on Bruker APEX II CCD diffractometer equipped with a graphite-monochromatized MoK α radiation source ($\lambda=0.71073$ Å). Empirical absorption was performed, and the structure was solved by direct methods and refined with the aid of a SHELXTL program package. All hydrogen atoms were calculated and refined using a riding model.

2.4. Magnetic susceptibility

The DC magnetic susceptibility measurements were made on an MPMS magnetometer at temperatures between 2.0 and 300 K. The pure polycrystalline samples were grounded into a fine powder to minimize possible anisotropic effects and loaded into gelatin capsules. The samples were cooled in a constant magnetic field of 50 Oe for measurements of magnetization versus temperature. The data were corrected for the susceptibility of the container and for the diamagnetic contribution from the ion core.

3. Results and discussion

The reactions between metal chloride (ZnCl₂, CoCl₂ and FeCl₃) and H₂BDC produced three 2D layered structures with the formula of (HTEA)₂[M₃(BDC)₃Cl₂] ($M=\text{Zn}^{2+}$ for **NTU-Z1a**, Co^{2+} for **NTU-Z1b**, and Fe^{2+} for **NTU-Z2**, TEA: triethylamine). Single crystal XRD analysis shows that **NTU-Z1a** crystallizes in the monoclinic space group *P21/n*. **NTU-Z1b** has the similar structure with **NTU-Z1a** while **NTU-Z2** crystallizes in the monoclinic space group *p21/c*. In **NTU-Z1a**, three Zn²⁺ ions are coordinated with carboxylates and chlorine atoms to form trinuclear Zn²⁺ clusters as the secondary building units (SBUs) (Fig. 2a). The trinuclear cluster has two crystallographically independent Zn²⁺ ions. The central Zn²⁺ ion is located at the inversion center and octahedrally coordinated with six O atoms from different carboxylate groups, while the terminal Zn atom is tetrahedrally connected with three O atoms from different carboxylate groups and one chloride ion.

In **NTU-Z2**, three Fe ions are bridged together to form a Fe trimeric cluster by six different carboxylate groups, where two μ_2 -O atoms from different carboxylates are found (Fig. 2b). Both terminal Fe ions in the cluster have one axial chloride ion, which is opposite to the Fe–Fe vector (Fig. 2b). The charges of Fe atom in **NTU-Z2** are +2, which is calculated from the charge balancing cations, indicating that an in situ reduction process occurred in the reaction system. There are two crystallographically independent Fe²⁺ ions in the trinuclear cluster. The configurations of the central Fe atom in cluster (located at inversion center) and two terminal Fe atoms are octahedral and five-coordinated modes, respectively.

The clusters in **NTU-Z1(a,b)** and **NTU-Z2** are interlinked together by BDC²⁻ ligands with different connectivity modes to form 2D layered structures (Figs. S1 and S2). Protonated HTEA⁺ molecules fill up the space between two layers as the charge

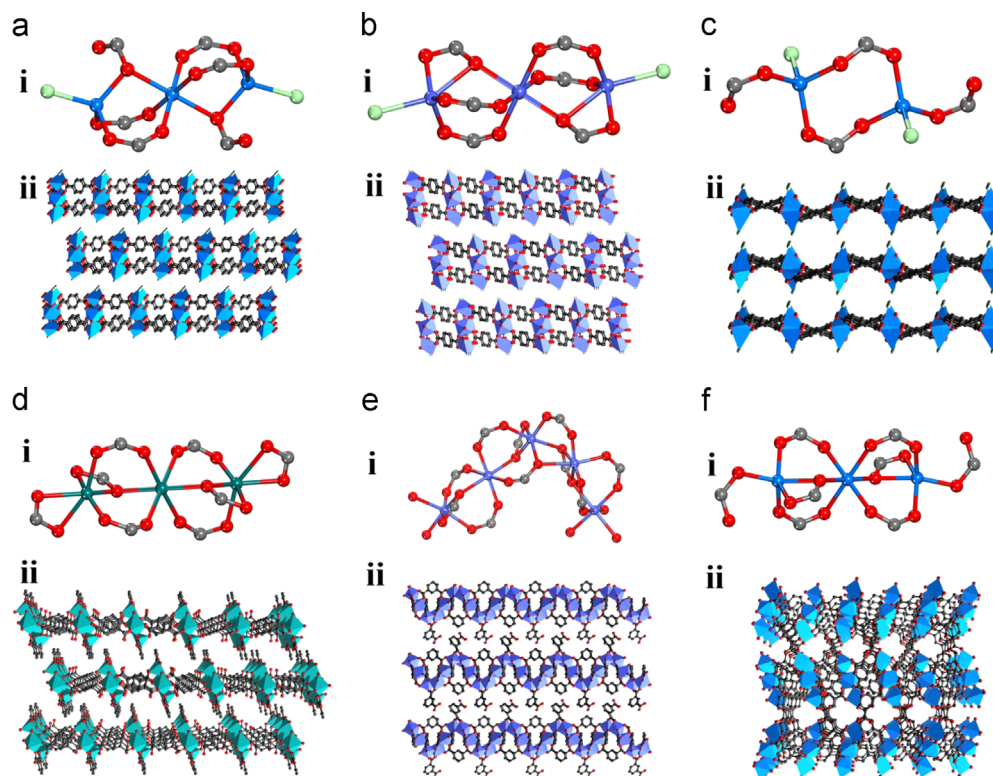


Fig. 2. (a) The SBUs in MOF **NTU-Z1a** (i), and 2D framework of **NTU-Z1a** viewed along the *b*-axis (ii). (b) The SBUs in MOF **NTU-Z2** (i), and 2D framework of **NTU-Z2** viewed along the *b*-axis (ii). (c) The SBUs in MOF **NTU-Z3** (i), and 2D framework of **NTU-Z3** viewed along the *b*-axis (ii). (d) The SBUs in MOF **NTU-Z4** (i), and 2D framework of **NTU-Z4** viewed along *a*-axis (ii). (e) The Fe²⁺ zigzag 1D chain in **NTU-Z5** (i) and the 2D layer structure in **NTU-Z5** viewed along the *b*-axis (ii). (f) The SBUs in MOF **NTU-Z6a** (i), and the 3D framework of **NTU-Z6a** viewed down the *b*-axis (ii). HTEA guests and H atoms were removed for clarity. C, O, Zn, Cd, Fe and Cl atoms are shown in gray, red, blue, green, purple and light green. (For interpretation of the references to color in this figure legend, the reader is referred to the web version of this article.)

balance cations. The nearest distances of $\text{Zn}^{2+} \cdots \text{Zn}^{2+}$, $\text{Co}^{2+} \cdots \text{Co}^{2+}$, and $\text{Fe}^{2+} \cdots \text{Fe}^{2+}$ are 3.26, 3.23 and 3.54 Å, respectively. Despite the similar molecular formula of **NTU-Z1(a,b)** and **NTU-Z2**, their coordination modes are very different. **NTU-Z1(a,b)** exhibits two distinct coordination modes of carboxylate: bidentate bridging $\mu_2\text{-}\eta^2$ mode (Fig. 1c) and bidentate bridging $\mu_2\text{-}\eta^1\text{:}\eta^1$ mode (Fig. 1d), while $\mu_2\text{-}\eta^1\text{:}\eta^1$ mode and $\mu_2\text{-}\eta^2\text{:}\eta^1$ mode (Fig. 1f) are found in **NTU-Z2**. Details of the crystal structure and refinement data are provided in supporting information (Table S1). The experimental powder XRD patterns for **NTU-Z1a**, **NTU-Z1b** and **NTU-Z2** match very well with the simulated ones (generated on the basis of single crystal structure analysis), which confirmed the phase purity of the bulk materials (Figure S8). TGA analysis indicated that **NTU-Z1** and **NTU-Z2** showed quite good thermal stability up to 310 °C (Fig. S10).

2D layered crystals **NTU-Z3** ((HTEA)[Zn(IPA)Cl]) were obtained from the reaction between ZnCl_2 and H_2IPA , which crystallizes in the Orthorhombic *Pbca* space group. The asymmetric unit contains one Zn^{2+} ion, one IPA^{2-} ligand, one chloride ion, and one protonated HTEA⁺ molecule. The Zn^{2+} ion is tetrahedrally connected to three carboxylate O atoms and one chlorine atom (Figs. 2c and S3). The carboxylate group in **NTU-Z3** shows two different coordination modes: monodentate η^1 mode (Fig. 1b) and bridging $\mu_2\text{-}\eta^1\text{:}\eta^1$ mode.

The reaction between CdCl_2 and H_2IPA produced **NTU-Z4** ((HTEA)₂[Cd₃(IPA)₄]), which crystallizes in the triclinic *P1* space group. All Cd^{2+} ions are octahedrally coordinated with O atoms of carboxylates to form trinuclear Cd^{2+} clusters (Fig. 2d). The trimeric clusters are interconnected through IPA^{2-} ligands to generate a 2D extended network with quadrangular channel dimensions of ca. 6.7×6.2 Å and 7.5×5.2 Å viewed along the *b*-axis and *a*-axis, respectively (Figs. 2d(ii) and S4). The space between two layers is occupied by guest HTEA⁺ molecules as the charge balance species. There are three different coordination modes of carboxylate groups in **NTU-Z4**: bridging $\mu_2\text{-}\eta^1\text{:}\eta^1$ mode, $\mu_2\text{-}\eta^2\text{:}\eta^1$ mode and chelating η^2 mode (Fig. 1e).

All Fe atoms are octahedrally coordinated with carboxylate groups to form 1D Fe^{2+} zigzag chains via corner and edge share in **NTU-Z5** ((HTEA)₂[Fe₃(IPA)₄]) (Fig. 2e). **NTU-Z5** crystallizes in the Orthorhombic *Pca2*(1) space group. The 1D zigzag chains are further connected together via IPA^{2-} ligands to generate a 2D layered structure (Figs. S5 and S6). Four different coordination modes of carboxylates to metal ions are found in **NTU-Z5**: $\mu_2\text{-}\eta^1\text{:}\eta^1$ mode, $\mu_2\text{-}\eta^2\text{:}\eta^1$ mode, tridentate bridging $\mu_3\text{-}\eta^1\text{:}\eta^2$ mode (Fig. 1g), and tetra-donor coordination $\mu_3\text{-}\eta^1\text{:}\eta^2\text{:}\eta^1$ mode (Fig. 1h).

NTU-Z6a ((HTEA)₂[Zn₃(IPA)₄]) was synthesized from the reaction of $\text{Zn}_5(\text{OH})_6(\text{CO}_3)_2$ and H_2IPA ligand, which crystallizes in the Orthorhombic *Pbca* space group. Five-connected and octahedrally coordinated Zn atoms are linked together through carboxylate group to form trinuclear Zn^{2+} clusters (Fig. 2f). Two crystalline independent IPA^{2-} ligands further link clusters together to form a 3D framework, where 1D channels with the dimensions of ca. 7.6×5.0 Å along the *b*-axis are observed. HTEA⁺ cations fill up these channels as charge balance species. **NTU-Z6a** has three different carboxylate coordination modes: monodentate η^1 mode, $\mu_2\text{-}\eta^1\text{:}\eta^1$ mode, and $\mu_2\text{-}\eta^2\text{:}\eta^1$ mode. The similar reaction between CoCl_2 and H_2IPA in PEG 200 produced the 3D framework of **NTU-Z6b** ((HTEA)₂[Co₃(IPA)₄]), which has the same structure with **NTU-Z6a**. TGA analysis indicated that **NTU-Z3**, **NTU-Z4**, **NTU-Z5** and **NTU-Z6(a,b)** showed quite good thermal stability (Fig. S11). After removing of cationic HTEA⁺ from the MOF crystals by heating, all the MOF structures were collapsed and no peak displayed in the powder XRD pattern. The Fe^{2+} -based MOFs **NTU-Z2** and **NTU-Z5** were not stable in air and decomposed when they were exposed in air for about one week. Other MOFs were quite stable in air and moisture.

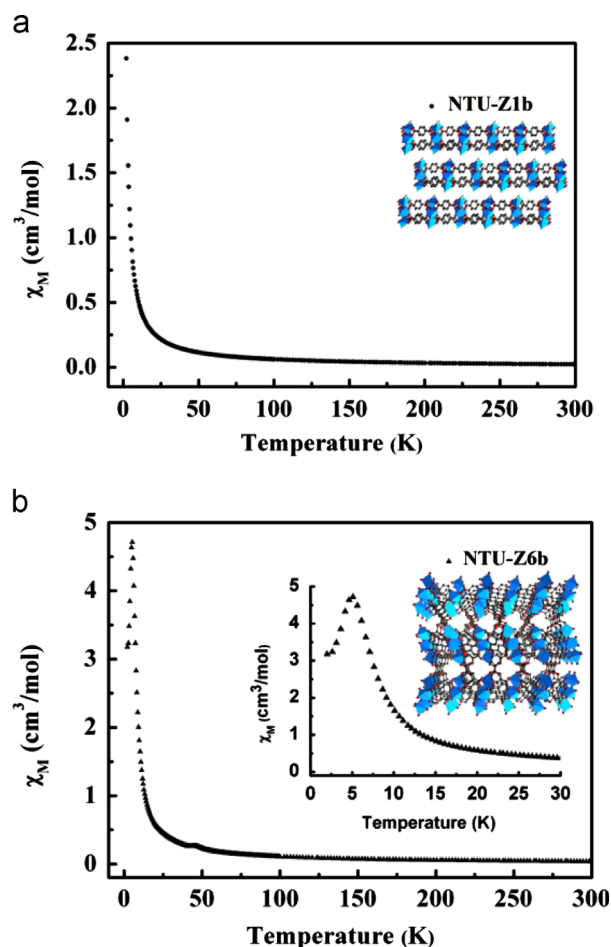


Fig. 3. Temperature dependence of magnetic susceptibility of **NTU-Z1b** and **NTU-Z6b**.

The magnetic properties of Co cluster-based MOFs have been studied for their potential applications as molecular magnets. [47–49] The magnetic susceptibility (χ_M) of Co-based 2D **NTU-Z1b** and 3D **NTU-Z6b** were measured in the temperature range of 2–300 K. As shown in Fig. 3a, the χ_M of **NTU-Z1b** obeys the Curie–Weiss law over the whole temperature range. The calculated Curie constant (*C*) and Weiss constant (θ) are $5.38 \text{ cm}^3 \text{ K mol}^{-1}$ and -0.25 K , indicating a weak antiferromagnetic interaction between the nearest magnetic Co^{2+} ions. The effective magnetic moment (μ_{eff}) for one Co^{2+} ion in **NTU-Z1b** is $3.79 \mu_B$. The magnetic behavior of **NTU-Z6b** displays a phase transition from paramagnetic to antiferromagnetic behavior when the temperature decreased to 5 K (Fig. 3b). The high temperature range ($T > 100 \text{ K}$) can be fitted with Curie–Weiss law with $C = 11.9 \text{ cm}^3 \text{ K mol}^{-1}$, and $\theta = -11.2 \text{ K}$. Although both **NTU-Z1b** and **NTU-Z6b** have trinuclear Co^{2+} clusters, the coordination configuration of Co^{2+} ions in **NTU-Z1b** and **NTU-Z6b** is different. Co^{2+} ions in **NTU-Z1b** have octahedral and tetrahedral coordinations while the Co^{2+} ions in **NTU-Z6b** possess octahedral coordination and five-coordination. The nearest distances of $\text{Co}^{2+} \cdots \text{Co}^{2+}$ in **NTU-Z1b** and **NTU-Z6b** are 3.23 and 3.41 Å, respectively. The different coordination modes of Co^{2+} ions in two MOFs may result in the different magnetic behaviors.

4. Conclusions

In conclusion, diverse crystalline MOFs have successfully been prepared using surfactant PEG-200 as reaction media and eight

different coordination modes of carboxylate groups in the as-prepared MOFs have been found. Co-based 2D **NTU-Z1b** shows a weak antiferromagnetic interaction between the nearest magnetic Co^{2+} ions while 3D **NTU-Z6b** displays a phase transition from paramagnetic to antiferromagnetic behavior at 5 K. Our result suggests that our strategy “growing crystalline materials in surfactants” could have great potential for the synthesis of novel MOFs with diverse structures.

Acknowledgment

Q.Z. acknowledges the financial support from AcRF Tier 1 (RG 18/09) and Tier 2 (ARC 20/12) from MOE, CREATE program (Nanomaterials for Energy and Water Management) from NRF, and New Initiative Fund from NTU, Singapore.

Appendix A. Supporting information

Supplementary data associated with this article can be found in the online version at <http://dx.doi.org/10.1016/j.jssc.2013.07.031>.

References

- [1] M.P. Suh, H.J. Park, T.K. Prasad, D.W. Lim, *Chem. Rev.* 112 (2012) 782–835.
- [2] K. Sumida, D.L. Rogow, J.A. Mason, T.M. McDonald, E.D. Bloch, Z.R. Herm, T.H. Bae, J.R. Long, *Chem. Rev.* 112 (2012) 724–781.
- [3] H.X. Deng, S. Grunder, K.E. Cordova, C. Valente, H. Furukawa, M. Hmadeh, F. Gandara, A.C. Whalley, Z. Liu, S. Asahina, H. Kazumori, M. O’Keeffe, O. Terasaki, J.F. Stoddart, O.M. Yaghi, *Science* 336 (2012) 1018–1023.
- [4] X.J. Wang, P.Z. Li, Y.F. Chen, Q. Zhang, H.C. Zhang, X.X. Chan, R. Ganguly, Y.X. Li, J.W. Jiang, Y.L. Zhao, *Sci. Rep.* 3 (2013) 1149, <http://dx.doi.org/10.1038/Srep01149>.
- [5] E.D. Bloch, W.L. Queen, R. Krishna, J.M. Zadrozny, C.M. Brown, J.R. Long, *Science* 335 (2012) 1606–1610.
- [6] J.R. Li, J. Sculley, H.C. Zhou, *Chem. Rev.* 112 (2012) 869–932.
- [7] S.C. Xiang, Z.J. Zhang, C.G. Zhao, K.L. Hong, X.B. Zhao, D.R. Ding, M.H. Xie, C.D. Wu, M.C. Das, R. Gill, K.M. Thomas, B.L. Chen, *Nat. Commun.* 2 (2011) 204, <http://dx.doi.org/10.1038/ncomms1206>.
- [8] J.K. Sun, M. Ji, C. Chen, W.G. Wang, P. Wang, R.P. Chen, J. Zhang, *Chem. Commun.* 49 (2013) 1624–1626.
- [9] M. Yoon, R. Srirambalaji, K. Kim, *Chem. Rev.* 112 (2012) 1196–1231.
- [10] A. Corma, H. Garcia, F.X.L. Xamena, *Chem. Rev.* 110 (2010) 4606–4655.
- [11] C. Wang, M. Zheng, W. Lin, *J. Phys. Chem. Lett.* 2 (2011) 1701–1709.
- [12] L.E. Kreno, K. Leong, O.K. Farha, M. Allendorf, R.P. Van Duyne, J.T. Hupp, *Chem. Rev.* 112 (2012) 1105–1125.
- [13] Y.J. Cui, Y.F. Yue, G.D. Qian, B.L. Chen, *Chem. Rev.* 112 (2012) 1126–1162.
- [14] Y.J. Cui, H. Xu, Y.F. Yue, Z.Y. Guo, J.C. Yu, Z.X. Chen, J.K. Gao, Y. Yang, G.D. Qian, B.L. Chen, *J. Am. Chem. Soc.* 134 (2012) 3979–3982.
- [15] Y. Kang, F. Wang, J. Zhang, X.H. Bu, *J. Am. Chem. Soc.* 134 (2012) 17881–17884.
- [16] J.C. Yu, Y.J. Cui, C.D. Wu, Y. Yang, Z.Y. Wang, M. O’Keeffe, B.L. Chen, G.D. Qian, *Angew. Chem. Int. Ed.* 51 (2012) 10542–10545.
- [17] H. Xu, X.T. Rao, J.K. Gao, J.C. Yu, Z.Q. Wang, Z.S. Dou, Y.J. Cui, Y. Yang, B.L. Chen, G.D. Qian, *Chem. Commun.* 48 (2012) 7377–7379.
- [18] P. Horcajada, R. Gref, T. Baati, P.K. Allan, G. Maurin, P. Couvreur, G. Férey, R.E. Morris, C. Serre, *Chem. Rev.* 112 (2012) 1232–1268.
- [19] A.C. McKinlay, R.E. Morris, P. Horcajada, G. Férey, R. Gref, P. Couvreur, C. Serre, *Angew. Chem. Int. Ed.* 49 (2010) 6260–6266.
- [20] P. Horcajada, T. Chalati, C. Serre, B. Gillet, C. Sebrie, T. Baati, J.F. Eubank, D. Heurtaux, P. Clayette, C. Kreuz, J.S. Chang, Y.K. Hwang, V. Marsaud, P.N. Bories, L. Cynober, S. Gil, G. Férey, P. Couvreur, R. Gref, *Nat. Mater.* 9 (2010) 172–178.
- [21] N. Stock, S. Biswas, *Chem. Rev.* 112 (2011) 933–969.
- [22] (a) C.-P. Li, M. Du, *Chem. Commun.* 47 (2011) 5958–5972;
(b) Q. Zhang, X. Bu, Z. Lin, T. Wu, P. Feng, *Inorg. Chem.* 47 (2008) 9724–9726.
- [23] (a) J. Zhang, J.T. Bu, S. Chen, T. Wu, S. Zheng, Y. Chen, R.A. Nieto, P. Feng, X. Bu, *Angew. Chem. Int. Ed.* 49 (2010) 8876–8879;
(b) Y. Liu, L.-M. Yu, S.C.J. Loo, R.G. Blair, Q. Zhang, *J. Solid State Chem.* 191 (2012) 283–286;
(c) Y. Liu, M.J.W. Tan, F. Wei, Y. Tian, T. Wu, C. Kloc, F. Huo, Q. Yan, H.H. Hng, J. Ma, Q. Zhang, *CrystEngComm* 41 (2012) 75–78.
- [24] J. Gao, S. Cao, Q. Tay, Y. Liu, L. Yu, K. Ye, P.C.S. Mun, Y. Li, G. Rakesh, S.C.J. Loo, Z. Chen, Y. Zhao, C. Xue, Q. Zhang, *Sci. Rep.* 3 (2013) 1853, <http://dx.doi.org/10.1038/srep01853>.
- [25] R.E. Morris, *Chem. Commun.* (2009) 2990–2998.
- [26] M.J. Earle, J.M.S.S. Esperanca, M.A. Gilea, J.N.C. Lopes, L.P.N. Rebelo, J.W. Magee, K.R. Seddon, J.A. Widegren, *Nature* 439 (2006) 831–834.
- [27] (a) Q. Zhang, I. Chung, J.I. Jang, J.B. Ketterson, M.G. Kanatzidis, *J. Am. Chem. Soc.* 131 (2009) 9896–9897;
(b) K. Biswas, Q. Zhang, I. Chung, J.-H. Song, J. Androulakis, A. Freeman, M. Kanatzidis, *J. Am. Chem. Soc.* 132 (2010) 14760–14762.
- [28] H. Fu, C. Qin, Y. Lu, Z.-M. Zhang, Y.-G. Li, Z.-M. Su, W.-L. Li, E.-B. Wang, *Angew. Chem. Int. Ed.* 51 (2012) 7985–7989.
- [29] J. Zhang, S.M. Chen, X.H. Bu, *Angew. Chem. Int. Ed.* 47 (2008) 5434–5437.
- [30] J.X. Liu, B. Lukose, O. Shekha, H.K. Arslan, P. Weidler, H. Gliemann, S. Brase, S. Grosjean, A. Godt, X.L. Feng, K. Mullen, I.B. Magdau, T. Heine, C. Woll, *Sci. Rep.* 2 (2012) 921, <http://dx.doi.org/10.1038/Srep00921>.
- [31] (a) Y. Yin, A.P. Alivisatos, *Nature* 437 (2005) 664–670;
(b) G. Lu, S.Z. Li, Z. Guo, O.K. Farha, B.G. Hauser, X.Y. Qi, Y. Wang, X. Wang, S.Y. Han, X.G. Liu, J.S. DuChene, H. Zhang, Q. Zhang, X.D. Chen, J. Ma, S.C. J. Loo, W.D. Wei, Y.H. Yang, J.T. Hupp, F.W. Huo, *Nat. Chem.* 4 (2012) 310–316;
(c) Y. Liu, F. Boey, L.L. Lao, H. Zhang, X. Liu, Q. Zhang, *Chem. Asian J.* 6 (2011) 1004–1006.
- [32] D. Sun, A.E. Riley, A.J. Cadby, E.K. Richman, S.D. Korlann, S.H. Tolbert, *Nature* 441 (2006) 1126–1130.
- [33] T. Brezesinski, J. Wang, J. Polleux, B. Dunn, S.H. Tolbert, *J. Am. Chem. Soc.* 131 (2009) 1802–1809.
- [34] K.E. Shopsowitz, H. Qi, W.Y. Hamad, M.J. MacLachlan, *Nature* 468 (2010) 422–U246.
- [35] J. Wei, Q. Yue, Z.K. Sun, Y.H. Deng, D.Y. Zhao, *Angew. Chem. Int. Ed.* 51 (2012) 6149–6153.
- [36] M. Guan, W.D. Wang, E.J. Henderson, O. Dag, C. Kubel, V.S.K. Chakravadhanula, J. Rinck, I.L. Moudrakovski, J. Thomson, J. McDowell, A.K. Powell, H.X. Zhang, G.A. Ozin, *J. Am. Chem. Soc.* 134 (2012) 8439–8446.
- [37] Y. Liu, J. Goebl, Y. Yin, *Chem. Soc. Rev.* 42 (2013) 2610–2653.
- [38] W.-W. Xiong, E.U. Athresh, Y.T. Ng, J. Ding, T. Wu, Q. Zhang, *J. Am. Chem. Soc.* 135 (2013) 1256–1259.
- [39] W.-W. Xiong, P.-Z. Li, T.-H. Zhou, A.I.Y. Tok, R. Xu, Y. Zhao, Q. Zhang, *Inorg. Chem.* 52 (2013) 4148–4150.
- [40] J. Gao, M. He, Z.Y. Lee, W. Cao, W.-W. Xiong, Y. Li, R. Ganguly, T. Wu, Q. Zhang, *Dalton Trans.* 42 (2013) 11367–11370.
- [41] C. Morelli, P. Maris, D. Sisci, E. Perrotta, E. Brunelli, I. Perrotta, M.L. Panno, A. Tagarelli, C. Versace, M.F. Casula, F. Testa, S. Ando, J.B. Nagy, L. Pasqua, *Nanoscale* 3 (2011) 3198–3207.
- [42] A. Dumas, C.D. Spicer, Z. Gao, T. Takehana, Y.A. Lin, T. Yasukochi, B.G. Davis, *Angew. Chem. Int. Ed.* 52 (2013) 3916–3921.
- [43] A. McPherson, *J. Biol. Chem.* 251 (1976) 6300–6303.
- [44] A. McPherson, *Methods* 34 (2004) 254–265.
- [45] G.J. Myatt, P.M. Budd, C. Price, F. Hollway, S.W. Carr, *Zeolites* 14 (1994) 190–197.
- [46] H. Sun, B.X. Shen, *Adsorption* 18 (2012) 103–111.
- [47] Z.M. Wang, K.L. Hu, S. Gao, H. Kobayashi, *Adv. Mater.* 22 (2010) 1526–1533.
- [48] M. Kurmoo, *Chem. Soc. Rev.* 38 (2009) 1353–1379.
- [49] R.X. Yao, X. Xu, X.M. Zhang, *Chem. Mater.* 24 (2012) 303–310.